Enhanced OTFS using Channel Modulation and Delay-Doppler Indexing

Nabarun Roy and A. Chockalingam
Department of ECE, Indian Institute of Science, Bangalore 560012

***Abstract*—Discrete Zak transform (DZT) based orthogonal time frequency space (OTFS) modulation provides robustness in high-mobility wireless channels and benefits in implementation complexity. Channel modulation (CM) and index modulation (IM) are promising physical layer techniques that offer improved spectral efficiencies and bit error performance. In this paper, we propose an OTFS-CM-IM scheme that integrates CM and delay-Doppler (DD) domain indexing that enhances the performance of DZT-OTFS. For the proposed OTFS-CM-IM scheme, we derive a compact input-output relation which enables system simulations and the computation of an upper bound on the bit error performance and the distance properties of the signal set. We consider two types of DD indexing, one with constellation indexing and one without. Our simulation results show that the proposed OTFS-CM-IM scheme performs better than the OTFS scheme (without CM and IM) and the OTFS-CM scheme (without IM). This enhanced performance is attributed to the improved distance properties of the proposed OTFS-CM-IM signal set.**

***Index Terms*—OTFS modulation, delay-Doppler domain, discrete Zak Transform, channel modulation, DD domain indexing, distance profile.**

I. Introduction

Future wireless communication systems are required to accommodate various emerging applications in high-mobility environments where the channels are both time dispersive and frequency dispersive. Orthogonal time frequency space (OTFS) modulation has emerged as a promising modulation scheme for such high-mobility scenarios. In OTFS, information symbols reside in the delay-Doppler (DD) domain, which experience a DD channel that changes slowly even when the channel is rapidly time varying. In the past research on OTFS, the conversion of transmission symbols from DD domain to time domain was carried out in two steps [1],[2], but recent research has proposed an alternate Zak transform approach for direct conversion of DD domain symbols into time domain [3]. Owing to the feasibility of practical implementation, discrete Zak transform based OTFS (DZT-OTFS) has been investigated recently [4]-[6]. In this paper, we propose a novel scheme to enhance the performance of DZT-OTFS by introducing channel modulation [7]-[9] and delay-Doppler indexing [10]-[12], which are promising physical layer techniques that offer improved spectral efficiencies and bit error performance.

DD domain indexing in an OTFS frame has been introduced in [10]. Block-wise index modulaiton (IM) schemes for OTFS named delay-IM OTFS (DeIM-OTFS) and Doppler-IM OTFS (DoIM-OTFS) have been introduced in [11], where a set of DD resource bins are activated simultaneously. Recent work presented in [12] proposes DD resource bin indexing along with indexing in the constellation sets. Distinct constellations are employed on various active resource blocks to enhance spectral efficiency. It is shown that bit error rate (BER) performance and rate of the DD domain indexed OTFS system is better than OTFS system without indexing. Channel modulation can be viewed as a transmission scheme that uses radio frequency (RF) mirrors to perturb the propagation environment in the near field of the transmit antenna to generate independent channel fade realizations at the receiver [7]-[9]. These fade realizations are used as the channel modulation alphabet. CM has the advantages of MIMO benefits at reduced RF hardware complexity and improved performance attributed to improved distance properties of the CM alphabet.

Inspired by the advantages of CM and DD domain indexing in OTFS, in this paper, we propose OTFS-CM-IM scheme which enhances the performance of OTFS using CM and DD domain IM, which has not been reported before. A summary of the new contributions in this paper is as follows.

- First, we develop an end-to-end input-output relation for the proposed OTFS-CM-IM scheme.
- We derive an upper bound on the BER performance of the proposed scheme under maximum likelihood (ML) detection. The upper bound is shown to be tight at high signal-to-noise ratios (SNRs).
- We analyze the BER performance through extensive simulations considering different system configuration settings and two types of DD domain IM schemes (namely, Type-I IM and Type-II IM) using minimum mean square error (MMSE) detection. Our simulation results show that 1) OTFS-CM-IM performs better than OTFS-CM and OTFS system without indexing and 2) Type-II IM with constellation indexing along with DD bin indexing further improves the BER performance of OTFS-CM-IM.

The rest of the paper is organized as follows. The considered system including the basic OTFS-IM system model is presented in Sec. II. The proposed OTFS-CM-IM scheme and the upper bound on BER are presented in Sec. III. Results and discussion are presented in Sec. IV. Conclusions and future work are presented in Sec. V.

Notations: Matrices and vectors are denoted by upper and lower case boldface letters, respectively, $\mathrm{diag}\{v_i\}$ denotes a diagonal matrix with diagonal entries $v_i, i = 1, 2, \cdots$, and $\mathbf{I}_K$ denotes the identity matrix of size K. $(\cdot)_N$ denotes the modulo N operation. Hermitian, transpose, and conjugation operations are denoted by $(\cdot)^H, (\cdot)^T$, and $(\cdot)^*$, respectively. Hadamard

This work was supported in part by the J. C. Bose National Fellowship, Department of Science and Technology, Government of India.

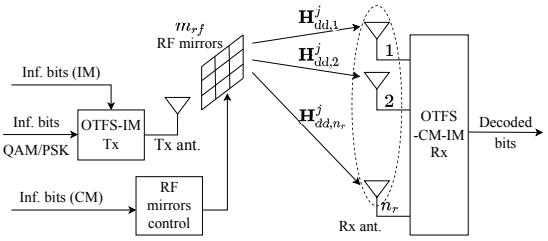

Fig. 1: Proposed OTFS-CM-IM scheme.

product, kronecker product, and convolution operations are denoted by $\odot, \otimes$ and $\circledast$, respectively.

II. System model

Fig. 1 shows the transceiver model of the proposed OTFS scheme with channel modulation and DD domain index modulation (OTFS-CM-IM). The transmitter consists of a single transmit antenna with m_{rf} RF mirrors placed near it. The m_{rf} RF mirrors are controlled using m_{rf} information bits. The receiver consists of n_r receive antennas. In this scheme, information bits are conveyed through 1) complex symbols from a modulation alphabet multiplexed in the DD grid, 2) index modulation of the DD bins, and 3) channel modulation alphabet (i.e., different channel fade realizations using m_{rf} RF mirrors). DZT-OTFS waveform [5],[6] is used. The OTFS-IM Tx conveys the bits of complex symbols and the DD index modulation bits. The CM alphabet bits are conveyed through the activation/deactivation of the RF mirrors. The OTFS-IM together with CM (realized using RF mirrors) constitute the proposed OTFS-CM-IM transmitter. We first present the system model considering OTFS-IM (in the following subsection) and then present the proposed OTFS-IM-CM scheme in the next section.

A. OTFS-IM system

The block diagram of OTFS-IM, assuming $n_r = 1$ receive antenna, is shown in Fig. 2. Based on the information bits, symbols from a modulation alphabet ($\mathbb{A}$) are multiplexed in an indexed DD grid of size $K \times L$, where K and L are the number of Doppler and delay bins respectively. Two different schemes of DD domain indexing are considered.

*1) Type-*I *indexing:* In this scheme of indexing, we partition the $K \times L$ DD grid into multiple blocks of size $u \times u$ and indexing is performed across the blocks. v DD bins in each $u \times u$ DD block are left idle and loaded with zero, while the remaining active DD bins in the block are loaded with information symbols from $\mathbb{A}$. b_{I} bits are carried by each block, among which $b_{1,\mathrm{I}}$ bits are used for DD index bin selection and $b_{2,\mathrm{I}} (= b_{\mathrm{I}} - b_{1,\mathrm{I}})$ bits are used for mounting symbols in the active DD bins. The rate achieved by this Type-I indexing scheme, in bits per channel use (bpcu), is given by

$$\eta_{\mathrm{IM_I}} = \frac{1}{u^2}\Big[\underbrace{\log_2 \binom{u^2}{v}}_{b_{1,\mathrm{I}} \text{ bits}} + \underbrace{(u^2 - v)\log_2 M}_{b_{2,\mathrm{I}} \text{ bits}}\Big], \tag{1}$$

where $M = |\mathbb{A}|$. Fig. 3 shows the OTFS block creator and the DD grid representation of this scheme of indexing.

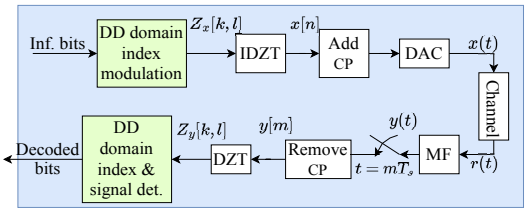

Fig. 2: OTFS-IM block diagram.

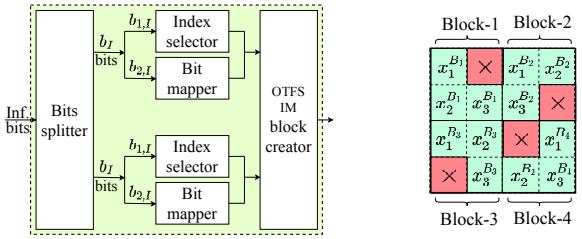

(a) DD domain index modulator (b) DD grid representation

Fig. 3: Type-I DD domain indexing.

*2) Type-*II *indexing:* In this scheme of indexing, the DD bins in each $u \times u$ DD block are indexed either along the delay axis or along the Doppler axis according to the DD selector bit ($b_{1,\mathrm{II}}$). v among u resource blocks (delay or Doppler blocks) are activated and information symbols from $\mathbb{A}$ are mounted along these blocks. The constellation $\mathbb{A}$ is rotated by different angles and a set of rotated constellations is generated with cardinality n_c. b_{II} bits are carried by each block, among which $b_{1,\mathrm{I}}$ bits are used for Delay/Doppler axis selection, $b_{2,\mathrm{I}}$ bits are used for resource blocks selection, $b_{3,\mathrm{I}}$ bits are used for constellation selection for each resource block, and $b_{4,\mathrm{I}}$ bits are used for mounting symbols in the activated resources. The rate achieved by this Type-II indexing scheme is given by

$$\eta_{\mathrm{IM_{II}}} = \frac{1}{u^2}\Big[\underbrace{1}_{b_{1,\mathrm{II}} \text{ bits}} + \underbrace{\log_2 \binom{u}{v}}_{b_{2,\mathrm{II}} \text{ bits}} + \underbrace{v \log_2 \binom{n_c}{1}}_{b_{3,\mathrm{II}} \text{ bits}} + \underbrace{uv \log_2 M}_{b_{4,\mathrm{I}} \text{ bits}}\Big]. \tag{2}$$

Fig. 4 shows the OTFS block creator and the DD grid representation of this scheme of indexing.

Input-output relation of OTFS-IM system: The OTFS-IM block creator integrates all the $(u \times u)$ blocks and generates the DD domain information symbols $\{Z_x[k,l] \in \mathbb{A}, k = 0, \cdots, K-1, l = 0, \cdots, L-1\}$ multiplexed over a $K \times L$ DD grid, where K and L are the number of Doppler and delay bins respectively. The $K \times L$ DD grid is defined as $\big\{\big(k\Delta\nu = \frac{k}{KLT_s}, l\Delta\tau = lT_s\big), k = 0, \cdots, K-1, l = 0, \cdots, L-1\big\}$, where $T_s = \frac{1}{B}$ is the symbol duration, B is the communication bandwidth, and $\Delta\tau = T_s$ and $\Delta\nu = \frac{1}{KLT_s}$ are the delay and Doppler resolutions, respectively. Using inverse DZT, the DD domain symbols are converted into time domain as

$$x[n] = \frac{1}{\sqrt{K}} \sum_{k=0}^{K-1} Z_x[k, (n)_L] e^{j2\pi \frac{\lfloor n/L \rfloor}{K}}. \tag{3}$$

To mitigate inter-frame interference, a cyclic prefix (CP) of length N_{CP} is appended. The discrete time sequence $x[n]$ is

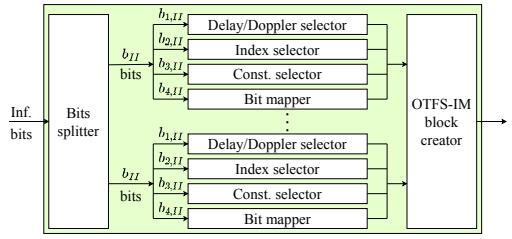

(a) DD domain index modulator

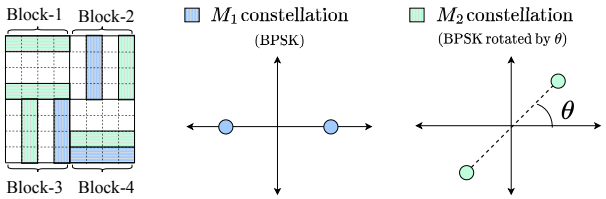

(b) DD grid representation with constellation sets

Fig. 4: Type-II DD domain indexing.

mounted over a continuous time transmit pulse $g_{tx}(t)$, $0 \leq t \leq T_s$ to obtain the continuous time domain signal $x(t)$ as

$$x(t) = \sum_{n=0}^{N+N_{\text{CP}}-1} x[(n-N_{\text{CP}})_N] g_{tx}(t-nT_s), \tag{4}$$

where $N = KL$ and $0 \leq t \leq (N+N_{\text{CP}})T_{\text{s}}$. The wireless channel is considered to be doubly selective in nature having P resolvable paths in the DD domain. The response of the channel in the DD domain is given by $h(\tau,\nu) = \sum_{i=1}^{P} h_i \delta(\tau-\tau_i)\delta(\nu-\nu_i)$, where h_i, τ_i, and ν_i are the channel coefficient, delay, and Doppler associated with the ith path, respectively. The ith path's delay is expressed as $\tau_i = (\alpha_i + a_i)T_{\text{s}}$, where α_i and $a_i \in (-0.5, 0.5]$ are the integer and fractional parts, respectively. Similarly, the ith path's Doppler is expressed as $\nu_i = \frac{(\beta_i + b_i)}{KLT_{\text{s}}}$, where β_i and $b_i \in (-0.5, 0.5]$ are the integer and fractional parts, respectively. The continuous time-domain signal $r(t)$ is at the receiver is given by

$$r(t) = \sum_{i=1}^{P} h_i \sum_{n=0}^{N+N_{\text{CP}}-1} x[(n-N_{\text{CP}}] g_{tx}(t-\tau_i-nT_s) e^{j2\pi\nu_i t} + w(t),$$

where $w(t)$ is the additive noise. The received signal $r(t)$ is matched filtered using the receive pulse $g_{rx}(t)$ (by assuming $g_{rx}(t) = g_{tx}(t)$ to be raised cosine pulse with roll-off factor γ). The matched filtered output $y(t)$ is sampled at $t = mT_s$, $m = 0, 1, \cdots, N + N_{\text{cp}} - 1$, and the N_{cp} samples corresponding to the CP are discarded. The resulting time-domain received sequence $y[m]$ can be expressed as [5]

$$y[m] = \sum_{i=1}^{P} h_i e^{j2\pi\tau_i\nu_i} \sum_{n=0}^{N-1} x[n] e_i[n] f_i[m-n] + v[m], \tag{5}$$

where $m, n = 0, \cdots, N-1$, $v[m]$ is the additive noise sample at the output of the matched filter operation, $e_i[n] = e^{j2\pi\frac{k_i}{KL}n}$, $k_i = NT_s\nu_i$, and $f_i[n] = \frac{\sin(\pi(n-l_i))}{\pi(n-l_i)} \frac{\cos(\gamma\pi(n-l_i))}{1-(2\gamma(n-l_i))^2}$, $l_i = \frac{\tau_i}{T_s}$. The sequences $e_i[n]$ and $f_i[n]$ account for the effect of delay and Doppler of the ith path. Using DZT, the received time sequence is converted into DD domain as

$$Z_y[k,l] = \frac{1}{\sqrt{K}} \sum_{n=0}^{K-1} y[l+nL] e^{-j2\pi\frac{k}{K}n}. \tag{6}$$

The DD domain input-output relation can be written as

$$\mathbf{y}_{\text{dd}} = \mathbf{x}_{\text{dd}}\mathbf{H}_{\text{dd}} + \mathbf{v}_{\text{dd}}, \tag{7}$$

where $\mathbf{x}_{\text{dd}}, \mathbf{y}_{\text{dd}}$, and $\mathbf{v}_{\text{dd}} \in \mathbb{C}^{1\times N}$ are vectorized column-wise such that $\mathbf{y}_{\text{dd}}(k+Kl) = Z_y[k,l]$, $\mathbf{x}_{\text{dd}}(k+Kl) = Z_x[k,l]$, $\mathbf{v}_{\text{dd}}(k+Kl) = Z_v[k,l]$ for $k = 0, \cdots, K-1$, $l = 0, \cdots, L-1$, and $Z_v[k,l]$ is the DZT of the noise sequence $v[m]$. The effective DD domain channel matrix $\mathbf{H}_{\text{dd}} \in \mathbb{C}^{N\times N}$ can be written in the form

$$\mathbf{H}_{\text{dd}} = \sum_{i=1}^{P} h_i^{'} \mathbf{E}_i \mathbf{G}_i, \tag{8}$$

where $h_i^{'} = h_i e^{j2\pi\tau_i\nu_i}$. The matrix $\mathbf{E}_i$ in (8) is a block diagonal matrix with matrices $\{\mathbf{B}_u\}_{u=1}^{L}$ along the diagonal, where $\mathbf{B}_u$ is a $K \times K$ matrix whose jth row is $\mathbf{B}_u[j-1,:] = (Z_{e_i}[:,u-1])^T \mathbf{P}_K^{j-1}$, $u = 1, \cdots, L$, $j = 1, \cdots, K$, Z_{e_i} is DZT of the sequence $e_i[n]$, and $\mathbf{P}_K$ is a $K \times K$ basic circulant permutation matrix (BCPM) [13]. The matrix $\mathbf{G}_i$ is an $N \times N$ matrix given by $\mathbf{G}_i = \begin{bmatrix} \mathbf{A}\mathbf{Q}_1 \\ \vdots \\ \mathbf{A}\mathbf{Q}_L \end{bmatrix}$, where $\mathbf{A}$ is a $K \times N$ block matrix given by $\mathbf{A} = [\text{diag}\{Z_{g_i}[:,0]\}, \cdots, \text{diag}\{Z_{g_i}[:,L-1]\}]$ with diag$\{\mathbf{c}\}$ denoting a diagonal matrix with elements of $\mathbf{c}$, Z_{g_i} is DZT of the sequence $e_i[n]$, and $\mathbf{Q}_u = \mathbf{P}_L^{u-1} \otimes \mathbf{I}_K$ be an $N \times N$ matrix, where $\mathbf{P}_L$ is an $L \times L$ BCPM and $\otimes$ operator denotes Kronecker product.

III. Proposed OTFS-CM-IM scheme and Analysis

In this section, we extend the OTFS-IM system model for $n_r \geq 1$ and introduce CM in the system model. For a given OTFS frame time, based on m_{rf} bits, a mirror activation pattern (MAP) is chosen among $N_m = 2^{m_{rf}}$ possible MAPs. Different MAPs result in different channel realizations having different coefficients but same DD values. The effective channel matrix $\bar{\mathbf{H}}_{\text{dd}} \in \mathbb{C}^{N_m N\times n_r N}$ can be expressed as

$$\bar{\mathbf{H}}_{\text{dd}} = \begin{bmatrix} \mathbf{H}_{\text{dd},1}^{1} & \mathbf{H}_{\text{dd},2}^{1} & \cdots & \mathbf{H}_{\text{dd},n_r}^{1} \\ \mathbf{H}_{\text{dd},1}^{2} & \mathbf{H}_{\text{dd},2}^{2} & \cdots & \mathbf{H}_{\text{dd},n_r}^{2} \\ \vdots & \vdots & \ddots & \vdots \\ \mathbf{H}_{\text{dd},1}^{N_m} & \mathbf{H}_{\text{dd},2}^{N_m} & \cdots & \mathbf{H}_{\text{dd},n_r}^{N_m} \end{bmatrix}, \tag{9}$$

where $\mathbf{H}_{\text{dd},i}^{j}$ denote the $N \times N$ channel matrix between the transmit antenna and the ith receive antenna ($i = 1, 2, \cdots, n_r$) corresponding to the jth MAP ($j = 1, 2, \cdots, N_m$), following the definition of the $\mathbf{H}_{\text{dd}}$ matrix in (8). The end-to-end input-output relation for OTFS-CM-IM can be expressed as

$$\bar{\mathbf{y}}_{\text{dd}} = \bar{\mathbf{x}}_{\text{dd}}\bar{\mathbf{H}}_{\text{dd}} + \bar{\mathbf{v}}_{\text{dd}}, \tag{10}$$

where $\bar{\mathbf{y}}_{\text{dd}}$, $\bar{\mathbf{v}}_{\text{dd}} \in \mathbb{C}^{1\times n_r N}$ are the received vector and noise vector, $\bar{\mathbf{x}}_{\text{dd}} \in \mathbb{C}^{1\times N_m N}$ is the OTFS-CM-IM transmit vector obtained by stacking $(N_m - 1)$ zero vectors each of size $1 \times N$, and OTFS-IM transmit vector $\mathbf{x}_{\text{dd}}$ of size $1 \times N$ as defined in (7) in the jth position as determined by m_{rf} bits, i.e.,

$$\bar{\mathbf{x}}_{\text{dd}} = \big[\mathbf{0}\ \mathbf{0}\ \cdots\ \underbrace{\mathbf{x}_{\text{dd}}}_{j\text{th position}}\ \cdots\ \mathbf{0}\ \mathbf{0}\big]. \tag{11}$$

Let C denote the number of blocks in an OTFS frame. Then, $C = \frac{KL}{u^2}$, where $K \times L$ OTFS frame is partitioned into $u \times u$ blocks. For Type-I indexing, the rate achieved is given by

$$\eta_{\text{I}} = \frac{1}{KL}\Big[C(\log_2 \binom{u^2}{v} + (u^2 - v)\log_2 M) + m_{rf}\Big]. \tag{12}$$

For Type-II indexing scheme, the rate achieved is given by

$$\eta_{\text{II}} = \frac{1}{KL}\Big[C(1 + \log_2 \binom{u}{v} + v\log_2 \binom{n_c}{1} + uv\log_2 M) + m_{rf})\Big]. \tag{13}$$

A. Upper bound on the ML performance of OTFS-CM-IM

The input-output relation of OTFS-IM system (as presented in (3)) can be reformulated as

$$\mathbf{y}_{\text{dd}} = \mathbf{h}\mathbf{X} + \mathbf{v}_{\text{dd}}, \tag{14}$$

where $\mathbf{X} = (\mathbf{I}_P \otimes \mathbf{x}_{\text{dd}})\begin{bmatrix}\mathbf{G}_1\mathbf{E}_1\\ \vdots \\ \mathbf{G}_P\mathbf{E}_P\end{bmatrix}$, and $\mathbf{h} = [h_1^{'}\ h_2^{'}\cdots h_P^{'}]$. Likewise OTFS-CM-IM model can be expressed as

$$\bar{\mathbf{y}}_{\text{dd}} = \bar{\mathbf{h}}\bar{\mathbf{X}} + \bar{\mathbf{v}}_{\text{dd}}, \tag{15}$$

where $\bar{\mathbf{h}} = [\mathbf{h}_1^1 \cdots \mathbf{h}_i^j \cdots \mathbf{h}_{n_r}^{N_m}]$, $\mathbf{h}_i^j$ represents the equivalent fade coefficient vector for ith receive antenna and jth MAP. $\bar{\mathbf{X}}$ is a $PN_m n_r \times Nn_r$ matrix expressed as

$$\bar{\mathbf{X}} = \mathbf{I}_{n_r} \otimes \tilde{\mathbf{X}}_{\text{dd}}\ ;\ \tilde{\mathbf{X}}_{\text{dd}} = \begin{bmatrix}\mathbf{Z}_0\\ \vdots \\ \mathbf{X} \\ \vdots \\ \mathbf{Z}_0\end{bmatrix} \leftarrow j\text{th position}, \tag{16}$$

where $\mathbf{Z}_0$ is a zero matrix of size $P \times N$ and $\mathbf{X}$ occupies the jth position in $\tilde{\mathbf{X}}_{\text{dd}}$ with j denoting the MAP index. The conditional pairwise error probability (PEP) between two distinct transmitted vectors $\bar{\mathbf{x}}_{\text{dd}}^p$ and $\bar{\mathbf{x}}_{\text{dd}}^q$ can be written as

$$\begin{aligned} P(\bar{\mathbf{x}}_{\text{dd}}^p \to \bar{\mathbf{x}}_{\text{dd}}^q|\bar{\mathbf{h}}) &= P(\|\bar{\mathbf{y}}_{\text{dd}} - \bar{\mathbf{h}}\bar{\mathbf{X}}_q\| < \|\bar{\mathbf{y}}_{\text{dd}} - \bar{\mathbf{h}}\bar{\mathbf{X}}_p\|) \\ &= \text{Q}\left(\sqrt{\frac{\|\bar{\mathbf{h}}(\bar{\mathbf{X}}_q - \bar{\mathbf{X}}_p)\|^2}{2N_0}}\right), \end{aligned} \tag{17}$$

where N_0 is the noise variance, and $\bar{\mathbf{X}}_p$ and $\bar{\mathbf{X}}_q$ are the equivalent matrix representations of $\bar{\mathbf{x}}_{\text{dd}}^p$ and $\bar{\mathbf{x}}_{\text{dd}}^q$, respectively. Using Chernoff bound, we can write

$$P(\bar{\mathbf{x}}_{\text{dd}}^p \to \bar{\mathbf{x}}_{\text{dd}}^q) \le \mathbb{E}_{\bar{\mathbf{h}}}\left\{\frac{1}{2}\exp\left(\frac{\|\bar{\mathbf{h}}(\bar{\mathbf{X}}_q - \bar{\mathbf{X}}_p)\|^2}{4N_0}\right)\right\}, \tag{18}$$

where $\mathbb{E}_{\bar{\mathbf{h}}}$ denotes the expectation operation over the random vector $\bar{\mathbf{h}}$. $\mathbf{h}_i^j$ is a unit energy random vector with its elements having identical and independent Gaussian distribution. Hence the elements of $\mathbf{h}_i^j$ have zero mean and $1/P$ variance. By applying SVD decomposition and taking expectation with respect to $\bar{\mathbf{h}}$, (18) can be simplified as

$$P(\bar{\mathbf{x}}_{\text{dd}}^p \to \bar{\mathbf{x}}_{\text{dd}}^q) \le \frac{1}{2}\prod_{l=1}^{r}\frac{1}{1 + \frac{\lambda_{lpq}}{4PN_0}}, \tag{19}$$

where r is the rank of $(\bar{\mathbf{X}}_q - \bar{\mathbf{X}}_p)$ and λ_{lpq} is the lth eigen value of $(\bar{\mathbf{X}}_q - \bar{\mathbf{X}}_p)(\bar{\mathbf{X}}_q - \bar{\mathbf{X}}_p)^H$. Using union bound, an upper bound on the BER of OTFS-CM-IM with ML detection can be obtained as

$$P_e \le \frac{1}{2^{KL\eta}}\sum_{p=1}^{Q}\sum_{q=1, q\neq p}^{Q}\delta(\bar{\mathbf{x}}_{\text{dd}}^p, \bar{\mathbf{x}}_{\text{dd}}^q)P(\bar{\mathbf{x}}_{\text{dd}}^p \to \bar{\mathbf{x}}_{\text{dd}}^q),$$

where $\delta(\bar{\mathbf{x}}_{\text{dd}}^p, \bar{\mathbf{x}}_{\text{dd}}^q)$ is the hamming distance between $\bar{\mathbf{x}}_{\text{dd}}^p$ and $\bar{\mathbf{x}}_{\text{dd}}^q$ and η is the rate of the OTFS-CM-IM system given by (12) for Type-I indexing and (13) for Type-II indexing.

B. Comparison of minimum distance of received signal sets:

The minimum euclidean distance among all pair of points in the received signal set for a given channel realization for OTFS-CM-IM system is given by

$$d^{\text{H}}_{\text{min,OTFS-CM-IM}} = \min_{\bar{\mathbf{x}}_{\text{dd}}^p, \bar{\mathbf{x}}_{\text{dd}}^q} \|\bar{\mathbf{x}}_{\text{dd}}^p\bar{\mathbf{H}}_{\text{dd}} - \bar{\mathbf{x}}_{\text{dd}}^q\bar{\mathbf{H}}_{\text{dd}}\|^2, \tag{20}$$

where $\bar{\mathbf{x}}_{\text{dd}}^p$ and $\bar{\mathbf{x}}_{\text{dd}}^q$ are chosen from all possible transmit vector of OTFS-CM-IM. As the channel matrix is random, we use Monte Carlo simulation to find the average minimum distance, denoted by $\tilde{d}_{\text{min,OTFS-CM-IM}}$, over a large number of channel realizations. Similarly, under same channel constraints (same number of paths, delays, Dopplers), let the minimum euclidean distance among all pair of points in the received signal set for OTFS-CM be denoted by $\tilde{d}_{\text{min,OTFS-CM}}$. Then, the SNR gap between the BER performance of these systems at high SNRs under ML detection can be analytically obtained as

$$\text{SNR}_{\text{gap}} = 20\log\left(\frac{\tilde{d}_{\text{min,OTFS-CM-IM}}}{\tilde{d}_{\text{min,OTFS-CM}}}\right)\ \text{dB}. \tag{21}$$

Remark on estimation of channel alphabet: For high Doppler channels, the time frequency domain channel response exhibits rapid variation, while the delay Doppler response of the channel exhibits slow variation. Because of this high coherence time in the delay Doppler domain, it becomes feasible to estimate the channel alphabet within this coherence time.

IV. Results and discussions

In this section, we present the simulated BER performance of the proposed OTFS-CM-IM system and compare it with that of OTFS and OTFS-CM systems

A. BER performance of OTFS-CM-IM with ML detection

First, we consider OTFS-CM-IM with small frame size ($K = L = 2$) for which ML detection is feasible. The bandwidth is set to 7.5 kHz (hence, $T_s = \frac{1}{B} = 0.133$ ms). The carrier frequency is set to 4 GHz. Fixing $\tau_p = 0.267$ ms (hence, $\nu_p = 3.75$ kHz) gives $\Delta\tau = \frac{\tau_p}{L} = 0.1335$ ms and $\Delta\nu = \frac{\nu_p}{K} = 1.875$ kHz as the delay and Doppler resolution, respectively. The DD block size considered for indexing is 2×2. For type-I indexing, one DD bin is left idle in the block and for type-II indexing, we activate one delay/Doppler resource block. m_{rf} is chosen to be 4. The considered channel has 4 paths (i.e., $P = 4$) with the DD profile in Table I.

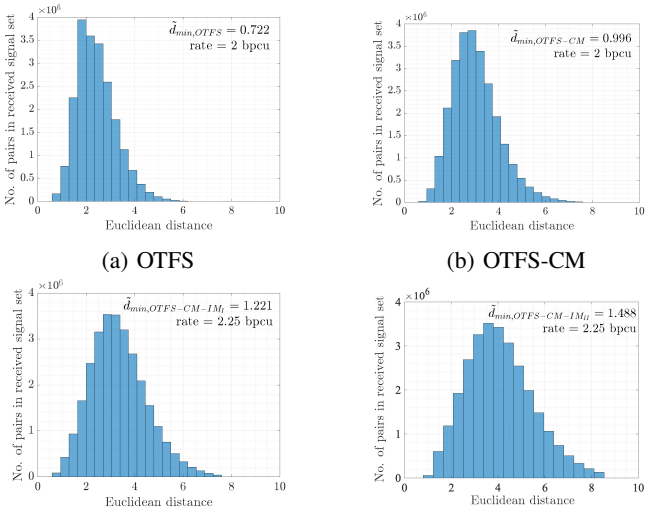

(a) OTFS (b) OTFS-CM

(c) OTFS-CM-IM$_{\mathrm{I}}$ (d) OTFS-CM-IM$_{\mathrm{II}}$

Fig. 5: Distance distribution for different signal sets.

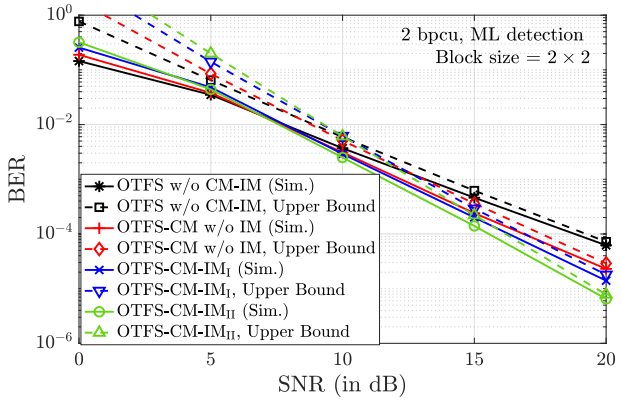

Fig. 6: BER performance of OTFS-CM-IM as a function of SNR under ML detection.

TABLE I: DD profile of the channel.

P (no. of paths)	τ (delay)	ν (Doppler)
4	$[0,\ 0,\ 1,\ 1]\ \Delta\tau$	$[0,\ 1,\ 0,\ 1]\ \Delta\nu$

For the system without CM and IM, the information symbols are chosen from 4-QAM alphabet and for OTFS-CM and OTFS-CM-IM$_{\mathrm{I}}$, the information symbols are chosen from BPSK alphabet. For OTFS-CM-IM$_{\mathrm{II}}$ system, number of distinct constellations (n_c) is 2. BPSK alphabet is chosen as the first constellation and the second constellation is obtained by rotating the BPSK alphabet by $\frac{\pi}{2}$.

Fig. 5 shows the distance distribution of the above mentioned systems with $n_r = 1$. The SNR gap between OTFS system without CM and OTFS-CM system at high SNRs can be computed to be $20\log\left(\frac{0.996}{0.722}\right) = 2.79$ dB. Similarly, at high SNRs, the SNR gap between OTFS-CM-IM$_{\mathrm{I}}$ and OTFS-CM system can be computed to be $20\log\left(\frac{1.221}{0.996}\right) = 1.77$ dB, and that between OTFS-CM-IM$_{\mathrm{II}}$ and OTFS-CM system can be computed to be $20\log\left(\frac{1.488}{0.996}\right) = 3.48$ dB. Fig. 6 shows the simulated BER with ML detection and the BER upper bounds, which are tight at high SNRs, validating the analysis.

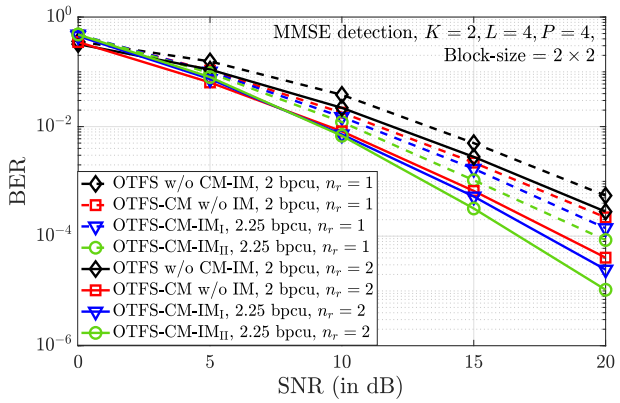

Fig. 7: BER performance of OTFS-CM-IM as a function of SNR for $n_r = 1, 2$ and $m_{rf} = 8$ under MMSE detection.

B. BER performance of OTFS-CM-IM with MMSE detection

OTFS frame size with $K = 2, L = 4$ is considered in Fig. 7. The (τ_p, ν_p) values, DD block indexing and the channel parameters are considered the same as in Fig. 6. $m_{rf} = 8$ RF mirrors and $n_r = 2$ receive antennas are used. Same constellations are used for each system as in Fig. 6. Fig. 7 shows that OTFS-CM performs better than OTFS without CM and the performance is further improved with DD domain indexing. Furthermore, constellation indexing along with DD domain indexing enhances the performance.

C. BER performance with large OTFS frame size

Large OTFS frame size with $K = L = 16$ is considered in Fig. 8, which is partitioned into blocks of size 2×2 for DD indexing. Fixing $\tau_p = 0.267$ ms gives $\nu_p = 3.75$ kHz. $m_{rf} = 8$ RF mirrors and $n_r = 8$ receive antennas are considered. The channel is considered to have $P = 4$ path with uniform power delay profile. For a given maximum delay $\tau_{\max}$ and maximum Doppler $\nu_{\max}$, the delay for the ith path is taken to be a random integer from uniformly sampled from $\left\{0, 1, \cdots, \text{round}\left(\frac{\tau_{\max}}{T_s}\right)\right\}$ and the ith path Doppler is taken as $\nu_{\max}\cos(\theta)$, where θ is uniformly distributed in $[-\pi, \pi]$. The $\tau_{\max}$ is taken to be $8T_s$ and $\nu_{\max}$ is taken to be 937 Hz. 4-QAM modulation alphabet is used in OTFS, OTFS-CM and OTFS-CM-IM$_{\mathrm{I}}$ system, while 4-QAM alphabet is rotated by $\frac{\pi}{8}$, $\frac{\pi}{4}$ and $\frac{3\pi}{8}$ to generate a set of four constellations for OTFS-CM-IM$_{\mathrm{II}}$ system (hence, $n_c = 4$). This ensures the same rate of 2 bpcu in all the systems. Fig. 8 shows that OTFS-CM-IM system outperforms both the OTFS-CM system and the conventional OTFS system without indexing.

V. Conclusions

In this work, we proposed a new OTFS-CM-IM scheme that enhanced the performance of the fundamental DZT-OTFS modulation in doubly-selective channels by using channel modulation and indexing in the delay Doppler grid. For the proposed OTFS-CM-IM scheme, we derived a compact end-to-end DD domain input-output relation, which serves as a foundational framework for exploring efficient techniques and

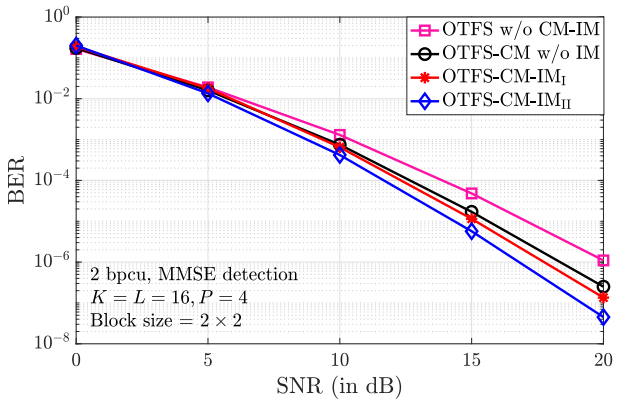

Fig. 8: BER performance of OTFS-CM-IM as a function of SNR for $n_r = 8$ and $m_{rf} = 8$ under MMSE detection.

algorithms in DZT-OTFS-based MBM transceivers. Furthermore, we utilized this input-output relation to establish an upper bound on the BER with ML detection. The upper bound was found to be tight at high SNRs. We also carried out a detailed BER performance evaluation through simulations for large frame sizes and higher-order QAM using MMSE detection. Our simulation results showed an SNR gain of about 1 dB to 3 dB in favour of OTFS-CM-IM compared to OTFS-CM and conventional OTFS scheme. This improved performance is due to the improved distance properties of the received OTFS-CM signal set. In this work, we have considered perfect knowledge of the channel. Channel estimation methods using machine learning techniques can be taken up as future work.

REFERENCES

[1] R. Hadani et al., "Orthogonal time frequency space modulation," *IEEE WCNC'2017*, pp. 1-6, Mar. 2017.

[2] Y. Hong, T. Thaj, and E. Viterbo, *Delay-Doppler Communications: Principles and Applications,* Academic Press, 2022.

[3] S. K. Mohammed, R. Hadani, A. Chockalingam, and R. Calderbank, "OTFS - A mathematical foundation for communication and radar sensing in the delay-Doppler Domain," *IEEE BITS the Information Theory Magazine*, vol. 2, no. 2, pp. 36-55, Nov. 2022.

[4] A. J. E. M. Janssen, "The Zak transform: a signal transform for sampled time-continuous signals," *Philips J. Res.*, 43, pp. 23-69, 1988.

[5] F. Lampel, A. Avarado, F. M. J. Willems, "On OTFS using the discrete Zak transform," *IEEE ICC'2022 Workshops*, pp. 729-734, May 2022.

[6] V. Yogesh, V. S. Bhat, S. R. Mattu, and A. Chockalingam, "On the bit error performance of OTFS modulation using discrete Zak transform," *IEEE ICC'2023*, pp. 741-746, May 2023.

[7] A. K. Khandani, "Media-based modulation: a new approach to wireless transmission," *IEEE ISIT'2013*, pp. 3050-3054, Jul. 2013.

[8] Y. Naresh and A. Chockalingam, "On media-based modulation using RF mirrors," *IEEE Trans. Veh. Tech.*, vol. 66, pp. 4967-4983, Jun. 2017.

[9] E. Basar and I. Altunbas, "Space-time channel modulation," *IEEE Trans. Veh. Tech.*, vol. 66, no. 8, pp. 7609-7614, Aug. 2017.

[10] Y. Liang, L. Li, P. Fan, and Y. Guan, "Doppler resilient orthogonal time- frequency space (OTFS) systems based on index modulation," *IEEE VTC'2020-Spring*, pp. 1-5, May-Jul. 2020.

[11] M. Qian *et al*, "Block-wise index modulation and receiver design for high-mobility OTFS communications," *IEEE Trans. Commun.*, vol. 71, no. 10, pp. 5726-5739, Oct. 2023.

[12] Y. I. Tek and E. Basar, "Joint delay-Doppler index modulation for orthogonal time frequency space modulation," *IEEE Trans. Commun.*, IEEE early access doi: 10.1109/TCOMM.2024.3370827.

[13] R. Horn and C. Johnson, *Matrix Analysis*, Cambridge Univ. Press, 2013.